Ultra-low loss Si_3N_4 waveguides with low nonlinearity and high power handling capability

Ming-Chun Tien,* Jared F. Bauters, Martijn J. R. Heck, Daniel J. Blumenthal and John E. Bowers

Department of Electrical and Computer Engineering, University of California, Santa Barbara, CA 93106, USA
**jtien@ece.ucsb.edu*

Abstract: We investigate the nonlinearity of ultra-low loss Si_3N_4-core and SiO_2-cladding rectangular waveguides. The nonlinearity is modeled using Maxwell's wave equation with a small amount of refractive index perturbation. Effective n_2 is used to describe the third-order nonlinearity, which is linearly proportional to the optical intensity. The effective n_2 measured using continuous-wave self-phase modulation shows agreement with the theoretical calculation. The waveguide with 2.8-μm wide and 80-nm thick Si_3N_4 core has low loss and high power handling capability, with an effective n_2 of about 9×10^{-16} cm^2/W.

OCIS codes: (250.4390) Nonlinear optics, integrated optics; (190.3270) Kerr effect; (260.2065) Effective medium theory.

References and links

1. A. Boskovic, S. V. Chernikov, J. R. Taylor, L. Gruner-Nielsen, and O. A. Levring, "Direct continuous-wave measurement of n_2 in various types of telecommunication fiber at 155 μm," Opt. Lett. **21**(24), 1966–1968 (1996).
2. Q. Lin, O. J. Painter, and G. P. Agrawal, "Nonlinear optical phenomena in silicon waveguides: modeling and applications," Opt. Express **15**(25), 16604–16644 (2007).
3. J. F. Bauters, M. J. R. Heck, D. John, M.-C. Tien, A. Leinse, R. G. Heideman, D. J. Blumenthal, and J. Bowers, "Ultra-low loss silica-based waveguides with millimeter bend radius," in *ECOC*(Torino, Italy, 2010).
4. R. S. Grant, "Effective non-linear coefficients of optical waveguides," Opt. Quantum Electron. **28**(9), 1161–1173 (1996).
5. C. Koos, L. Jacome, C. Poulton, J. Leuthold, and W. Freude, "Nonlinear silicon-on-insulator waveguides for all-optical signal processing," Opt. Express **15**(10), 5976–5990 (2007).
6. K. Okamoto, *Fundamentals of optical waveguides* (Academic Press, 2006).
7. A. B. Fallahkhair, K. S. Li, and T. E. Murphy, "Vector finite difference modesolver for anisotropic dielectric waveguides," J. Lightwave Technol. **26**(11), 1423–1431 (2008).
8. S. V. Chernikov, and J. R. Taylor, "Measurement of normalization factor of $n_{(2)}$ for random polarization in optical fibers," Opt. Lett. **21**(19), 1559–1561 (1996).
9. A. Lamminpaa, T. Niemi, E. Ikonen, P. Marttila, and H. Ludvigsen, ""Effects of dispersion on nonlinearity measurement of optical fibers," Opt. Fiber Technol," Mater. Devices Syst. **11**, 278–285 (2005).
10. K. Ikeda, R. E. Saperstein, N. Alic, and Y. Fainman, "Thermal and Kerr nonlinear properties of plasma-deposited silicon nitride/ silicon dioxide waveguides," Opt. Express **16**(17), 12987–12994 (2008).
11. H. Schmidt, M. Gupta, and M. Bruns, "Nitrogen diffusion in amorphous silicon nitride isotope multilayers probed by neutron reflectometry," Phys. Rev. Lett. **96**(5), 055901 (2006).

1. Introduction

Ultra-low loss waveguides are required for many applications, such as integrated optical delay lines, optical buffers, and high-Q resonators, which play important roles for planar lightwave circuits (PLC). As the waveguide loss decreases and thus allows longer propagation lengths, the nonlinear effect will accumulate and show up even with relatively low input optical power and eventually affect the performance of the PLC. This is especially important for devices that need highly accurate phase control. Therefore, it is essential to know the nonlinear coefficient of waveguides to predict the performance.

#133525 - $15.00 USD Received 17 Aug 2010; revised 22 Oct 2010; accepted 22 Oct 2010; published 26 Oct 2010

In this paper, we focus on the application of on-chip optical delay lines, where low-nonlinearity material is required for optical waveguide design. Silica-based material is a good candidate because of its lower nonlinearity and optical loss compared to silicon [1,2]. We have demonstrated ultra-low loss of 3 dB/m in Si_3N_4-core and SiO_2-cladding rectangular waveguides with 2-mm bend radius [3]. Here, we investigate the third-order nonlinearity of the waveguides, and the resulting power handling capability. When the optical mode is mostly confined in the core of the waveguides, the core contributes most of the nonlinearity. However, if the optical mode is distributed in the core and cladding region, an effective n_2 is used to consider the nonlinearity from both cladding and core. Ref [4]. has derived the formula of effective n_2 for low-index contrast waveguide ($n_{core} \approx n_{clad} \approx n_{eff}$), such as optical fibers. However, the formula is not applicable for high-index-contrast waveguides, such as silicon or silicon nitride waveguides. Therefore, we derive the effective n_2 by solving Maxwell's wave equation with introduced index perturbation due to the nonlinearity. This method is also compared to ref [5], which uses vectorial mode solver and nonlinear propagating equations to obtain effective nonlinearity. Finally, a general nonlinear waveguide can be modeled using an effective n_2, and thus the nonlinear effect can be engineered through proper waveguide design.

2. Effective n_2 coefficient

The response of materials becomes nonlinear at high intensities. The third-order nonlinearity, which comes mostly from the dielectric Kerr effect, is linearly proportional to optical intensity. The resulting refractive index change of waveguides can be expressed by

$$\Delta n = n_{2,eff} I_{eff} = n_{2,eff} \frac{P_{tot}}{A_{eff}}, \tag{1}$$

$$\text{where } A_{eff} = \frac{\left(\iint I(x,y)dxdy\right)^2}{\iint I(x,y)^2 dxdy}. \tag{2}$$

$n_{2,eff}$ is the effective nonlinear refractive index coefficient, I_{eff} is average optical intensity of the effective core area, P_{tot} is total optical power, and $I(x,y)$ is the intensity distribution. The effective core area, A_{eff}, is used to indicate how well the optical mode is confined in the core and the corresponding effective mode size. The schematic of the waveguide is shown in Fig. 1(a). In a large-core waveguide, most of the optical power is confined in the core, and thus the nonlinearity of the core dominates. As a result, the effective n_2 of the waveguide is close to n_2 of the core. In nano-core Si_3N_4 waveguides, the optical power is weakly confined in the core (Fig. 1(b)); therefore, it is necessary to consider the nonlinearity from both the Si_3N_4 core and the SiO_2 cladding, and thus the effective n_2 falls between the nonlinear refractive index coefficients of the core and the cladding.

In order to obtain the effective n_2 of waveguides, we solve Maxwell's wave equation with introduced power-dependent refractive index change of the waveguide due to the nonlinearity. Since the refractive index change is relatively small, we use a perturbation method [6] to introduce the small amount of index change. The refractive index distribution for the waveguide is written as

$$n(x,y)^2 = \left(n_0(x,y) + n_2(x,y)I(x,y)\right)^2 \approx n_0(x,y)^2 + 2n_0(x,y)n_2(x,y)I(x,y), \tag{3}$$

where n_0 is the linear material refractive index. For quasi-TE modes in a rectangular waveguide, the wave equation is expressed as

$$\nabla^2 H_y + \left(k^2 n(x,y)^2 - \beta^2\right) H_y = 0, \tag{4}$$

#133525 - $15.00 USD Received 17 Aug 2010; revised 22 Oct 2010; accepted 22 Oct 2010; published 26 Oct 2010

where k is the free-space wavevector and β is the propagation constant. The magnetic field H_y and eigenvalue β^2 of the above equation are expressed in the first-order perturbation form as

$$H_y = H_{y0} + \Delta H_{y1} \tag{5}$$

$$\beta^2 = \beta_0^2 + \Delta\beta_1^2. \tag{6}$$

Substituting Eq. (3), (5), and (6) into (4) and simplifying the equation using Green's theorem, we obtain

$$\Delta\beta_1^2 = \frac{k^2 \iint 2n_0(x,y)n_2(x,y)I(x,y)^2 dxdy}{\iint I(x,y)dxdy}. \tag{7}$$

From the definition of the propagation constant, Eq. (6) can also be expressed as

$$\beta^2 = \left(n_{0,eff} + n_{2,eff} I_{eff}\right)^2 k^2 \approx \beta_0^2 + 2n_{0,eff} n_{2,eff} I_{eff} k^2, \tag{8}$$

where $n_{0,eff}$ is the effective linear index of the waveguide, and I_{eff} is average optical intensity of the effective core area defined by

$$I_{eff} = \frac{P_{tot}}{A_{eff}} = \frac{\iint I(x,y)^2 dxdy}{\iint I(x,y)dxdy}. \tag{9}$$

Comparing Eq. (6), (7), and (8), the effective n_2 is then obtained as follows.

$$n_{2,eff} = \frac{\iint n_0(x,y)n_2(x,y)I(x,y)^2 dxdy}{n_{0,eff}\iint I(x,y)^2 dxdy}. \tag{10}$$

For a waveguide with step-index difference as illustrated in Fig. 1(a), we define confinement factors for nonlinearity as follows.

$$\begin{aligned} \Gamma_{core} &= \frac{\iint_{core} I(x,y)^2 dxdy}{\iint_{\infty} I(x,y)^2 dxdy} \\ \Gamma_{clad} &= \frac{\iint_{clad} I(x,y)^2 dxdy}{\iint_{\infty} I(x,y)^2 dxdy}. \end{aligned} \tag{11}$$

The effective n_2 is then expressed in a simple way as

$$n_{2,eff} = \frac{n_{0,core} n_{2,core} \Gamma_{core} + n_{0,clad} n_{2,clad} \Gamma_{clad}}{n_{0,eff}}. \tag{12}$$

#133525 - $15.00 USD Received 17 Aug 2010; revised 22 Oct 2010; accepted 22 Oct 2010; published 26 Oct 2010

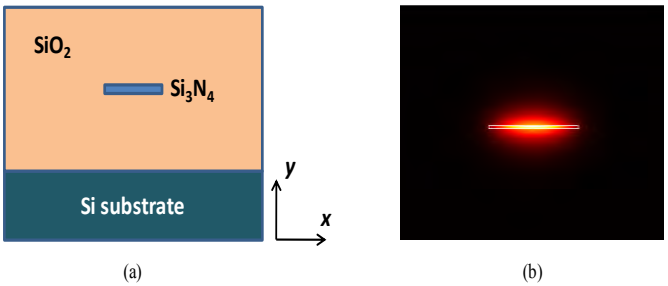

Fig. 1. (a) Schematic of a channel waveguide with Si_3N_4 core and SiO_2 cladding. (b) Calculated TE fundamental mode profile of the channel waveguide. The dimension of the Si_3N_4 core is 2.8 μm by 80 nm.

We compare this analytic perturbation method with the conventional scalar method [4] and the fully vectorial numerical method [5] via the nonlinear parameter $\gamma = \frac{2\pi}{\lambda}\frac{n_{2,eff}}{A_{eff}}$. The analytic perturbation method and conventional scalar method are implemented by using the Marcatili's method [6] to solve the electrical and magnetic field distributions while the numerical method is incorporated into MATLAB with vertorial finite-difference algorithm [7]. The nonlinearity of the waveguides with various Si_3N_4 core thicknesses is calculated using these three methods and shown in Fig. 2. When the core thickness is reduced and sufficiently small, the calculated results become similar because the optical mode is weakly guided. The waveguide nonlinearity measured by self-phase modulation (SPM), which will be described in Section 3, is also included for comparison.

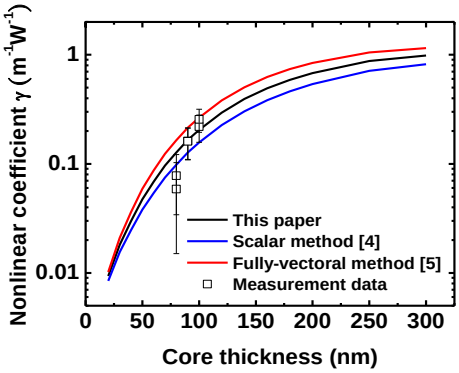

Fig. 2. Calculated nonlinear coefficient γ of channel waveguides with various Si_3N_4 core thicknesses using different methods. The measured nonlinearity is also included for comparison.

3. Measurement of waveguide nonlinearity

Channel waveguides with Si_3N_4 core and SiO_2 cladding are fabricated with LioniX BV's TriPleX^{TM} LPCVD technology. The Si_3N_4 cores are 2.8-μm wide and 80-nm to 100-nm thick with 8-μm-thick upper and lower SiO_2 cladding. The whole waveguides are built on silicon substrates. In order to characterize the nonlinear effect of the channel waveguides, we measure the nonlinear phase shift induced by the continuous-wave (CW) SPM [1,8,9] for different launched optical powers in the waveguide. The measurement setup is illustrated in Fig. 3. Two distributed feedback (DFB) lasers with wavelengths separated by about 0.4 nm are coupled to a 3-dB coupler to generate a beat signal of 50 GHz. The power of the lasers is set the same by a variable optical attenuator, and the lasers are adjusted to be copolarized by

#133525 - $15.00 USD Received 17 Aug 2010; revised 22 Oct 2010; accepted 22 Oct 2010; published 26 Oct 2010

the polarization controllers on both arms. The beat signal is then amplified by an erbium-doped fiber amplifier (EDFA) with 33-dBm maximum output power to generate sufficient optical intensity for observing the nonlinear effect. The power is coupled into and out of the waveguide through lensed fibers. The optical spectrum due to SPM is analyzed by an optical spectrum analyzer while the power is measured by a power meter.

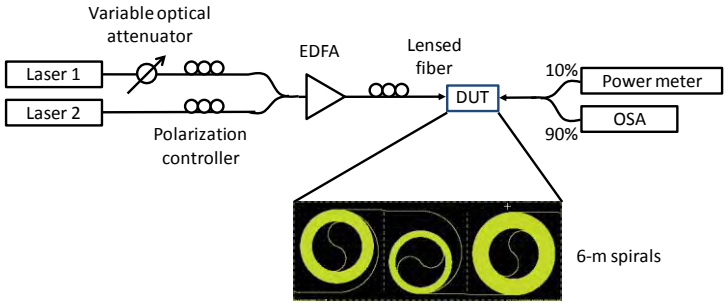

Fig. 3. Nonlinearity measurement setup using CW SPM method.

A measured SPM spectrum for TE-polarized light through a 6-m long spiral waveguide is shown in Fig. 4. With 29-dBm beat signals launched into the waveguide, the nonlinear effect is observed through the spectrum. The nonlinear phase shift is extracted from the relative intensity of the fundamental wavelength and the first-order sideband. The relation between the nonlinear phase shift and the intensity is given as [1]

$$\frac{I_0}{I_1} = \frac{J_0^2(\varphi_{SPM}/2) + J_1^2(\varphi_{SPM}/2)}{J_1^2(\varphi_{SPM}/2) + J_2^2(\varphi_{SPM}/2)}, \tag{13}$$

where I_0 and I_1 are the intensities of the fundamental wavelength and the first-order sideband, J_n is the Bessel function of the *nth* order, and φ_{SPM} is the nonlinear phase shift due to SPM. The phase shift only depends on the intensity ratio between the fundamental wavelength and the first-order sideband. It is independent of the laser linewidth and the wavelength separation of the two lasers if the chromatic dispersion is negligible. To neglect the chromatic dispersion, the wavelength separation and the waveguide length must be small enough [1,9]. We also experimentally confirmed the influence of dispersion is negligible by tuning the wavelength separation of the lasers.

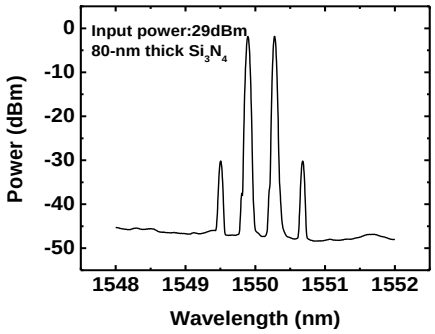

Fig. 4. SPM spectrum through a 6-m long spiral waveguide with 2.8 μm of core width and 80 nm of core thickness. The input light is TE-polarized with optical power of 29 dBm.

The relation between the nonlinear phase shift and input optical power for three test chips with different waveguide core thicknesses (80 nm, 90 nm, and 100 nm) is shown in Fig. 5. It should be mentioned that the nonlinearity from the EDFA was measured and subtracted when

#133525 - $15.00 USD Received 17 Aug 2010; revised 22 Oct 2010; accepted 22 Oct 2010; published 26 Oct 2010

characterizing the waveguide nonlinearity. The waveguide with thicker core exhibits larger nonlinear phase shift because of its smaller effective core area and thus stronger intensity.

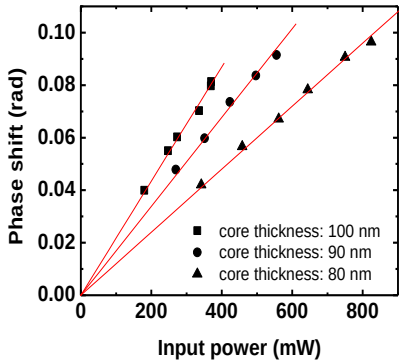

Fig. 5. Measured nonlinear phase shifts at various input powers for different Si_3N_4 core thicknesses. The solid lines are linear fitting of the measurements.

Once the nonlinear phase shift is known, the nonlinear coefficient γ and effective n_2 are derived from the slope of the fitted straight lines in Fig. 5, and plotted in Fig. 2 and Fig. 6 using the following formula [8].

$$\varphi_{SPM} = \frac{2\pi}{\lambda}\frac{n_{2,eff}}{A_{eff}} L_{eff} P_{in} = \gamma L_{eff} P_{in}, \tag{14}$$

where P_{in} is the waveguide input power and L_{eff} is the effective length defined as

$$L_{eff} = \frac{\left(1 - e^{-\alpha L}\right)}{\alpha}, \tag{15}$$

where L is the actual length of the waveguide and α is the waveguide loss. The squares in Fig. 2 and Fig. 6 are measurement data points from six test chips with three different Si_3N_4 core thicknesses while the solid lines represent the calculated nonlinearity as described in Section 2. The nonlinear refractive index coefficients n_2 for Si_3N_4 and SiO_2 are 3.5×10^{-15} cm^2/W and 2×10^{-16} cm^2/W, respectively, for calculation [1,10]. When the core thickness is reduced, the optical mode of the waveguide is squeezed out and more optical power overlaps with the SiO_2 cladding. Therefore, the effective n_2 is closer to n_2 of SiO_2 with reduced core thickness. The measured γ and effective n_2 are a little less than the theoretical prediction because a thin silicon oxynitride layer may occur at the interface of Si_3N_4 and SiO_2 because of nitrogen diffusion during the thermal annealing step of waveguide fabrication [11]. This influence is more obvious especially for a very thin Si_3N_4 layer. It should also be mentioned that all the waveguide nonlinearity is measured with TE-polarized optical input because the waveguide is designed to support fundamental TE mode only. The loss of TM mode is much larger than that of TE mode; therefore, it is not possible to characterize the waveguide nonlinearity with TM-polarized optical input.

#133525 - $15.00 USD Received 17 Aug 2010; revised 22 Oct 2010; accepted 22 Oct 2010; published 26 Oct 2010

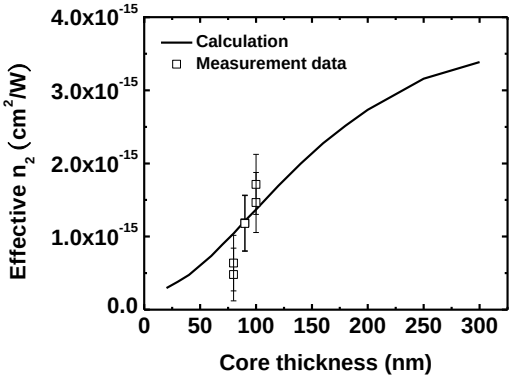

Fig. 6. Effective n_2 for different core thicknesses. The solid lines represent the theoretical calculation using the perturbation theory while the squares represent the measured data points.

For the application of optical delay lines, low nonlinearity is required to have small power-dependent optical phase variation over a length of waveguide. Given a specific phase variation tolerance, we can estimate the maximum handling power for a waveguide. For our 80-nm-thick Si_3N_4 waveguides, the maximum affordable propagation power over 20-m long waveguides (100-ns delay) can be as large as 120 mW with phase variation less than $\pi/20$. It is feasible to propagate even higher power by reducing Si_3N_4-core thickness in order to lower the nonlinearity of waveguides, as indicated in Fig. 6.

4. Conclusions

We have demonstrated ultra-low loss Si_3N_4-core and SiO_2-cladding rectangular waveguides that are capable of handling high propagating power because of their low nonlinearity. The nonlinearity of the waveguide is described using effective n_2, which is derived by solving Maxwell's wave equation with introduced power-dependent refractive index perturbation. The effective n_2 of the waveguides with different core thicknesses is measured using CW SPM and shows agreement with the theoretical calculation of waveguide nonlinearity. The waveguide with 80-nm-thick core is characterized, and has effective n_2 of about 9×10^{-16} cm^2/W, which can handle 120-mW optical power over a length of 20 meters with negligible power-dependent phase variation.

Acknowledgements

The authors thank Scott Rodgers, Daoxin Dai, Zhi Wang, and Paolo Pintus for helpful discussions. This work is supported by DARPA MTO under iPhoD contract No: HR0011-09-C-0123.

#133525 - $15.00 USD Received 17 Aug 2010; revised 22 Oct 2010; accepted 22 Oct 2010; published 26 Oct 2010